01.78.10

Radiation Effects
1978, Vol. 36, pp. 73–82

© Gordon and Breach Science Publishers Ltd., 1978
Printed in Great Britain

C.N.E.A. Biblioteca
ARCHIVO PUBLICACIONES
Nº 1 AÑO 1978

THE RECRYSTALLIZATION OF ION-IMPLANTED SILICON LAYERS
II. Implant Species Effect

C. E. CHRISTODOULIDES,† R. A. BARAGIOLA,†‡ D. CHIVERS,§ W. A. GRANT† and J. S. WILLIAMS||

†*Department of Electrical Engineering, University of Salford, Salford M5 4WT, England,* §*Chemistry Division, A.E.R.E. Harwell, Oxon., England,* ||*Institute of Physics, University of Aarthus, DK-8000 Aarhus C, Denmark*

(*Received October 24, 1977*)

Rutherford backscattering and channeling (RBS) has been employed to investigate the annealing characteristics of ion-bombarded ⟨111⟩ silicon for a wide range of implant species. The general recrystallization behaviour is that high levels of remnant disorder are observed for high-dose (typically $> 10^{15}$ ions cm^{-2}) implants of all species investigated, and transmission electron microscopy indicates the presence of a polycrystalline reordered layer in such cases. The magnitude of the remnant disorder (misorientation of grains with respect to the underlying bulk substrate) is observed to increase with both implant dose and original amorphous-layer thickness and to exhibit a slight implant-mass dependence. Although the recrystallization behaviour is qualitatively similar for all species studied, certain species (mainly those soluble in silicon) are found to influence the regrowth process at low implant concentrations. It is suggested that stress/strain effects, attributed to high implanted concentrations, play a major role in the inhibition of epitaxial silicon recrystallization but that species effects can become dominant at lower implant concentrations.

1 INTRODUCTION

In the first article[1] of the current series on silicon recrystallization, it was established that silicon surface layers, rendered amorphous by high-dose Pb^+-implantation (typically $> 5 \times 10^{14}$ cm^{-2} at 20 keV), reorder as a polycrystalline network, where the degree of polycrystallinity (i.e., misorientation of grains with respect to the underlying substrate) increases with increasing Pb^+ dose. The observed dose dependence[1,2] of recrystallization suggested that epitaxial recovery of Pb^+-implanted silicon was inhibited by high implant concentrations. Moreover, detailed Rutherford-backscattering (RBS) and transmission electron-microscopy (TEM) investigations indicated that the reordered silicon structure was dependent upon the local Pb concentration encountered as crystalline regrowth progressed from the underlying bulk lattice towards the silicon surface. Implantation-induced stress/strain within the near-surface was recently suggested[3] as a likely cause of the observed poor epitaxial recovery of high-dose-implanted silicon.

Other reported observations of the annealing behaviour of silicon implanted with a wide range of different species appear to be consistent with details of the recrystallization representation outlined above. For example, high levels of residual disorder in annealed silicon,[4–9] evidence for a polycrystalline reordered structure,[9–11] a dose dependence of recrystallization,[6–8] and outdiffusion of implant species during or following lattice reordering[8,12,13] are all aspects of the Pb^+-implanted silicon behaviour. However, because of the large number of parameters, which appear to play a role in epitaxial regrowth, and the differences in experimental approach adopted by the various workers, it is difficult to compare and evaluate the body of data reported in the literature. Therefore, in the present study, the annealing behaviour of amorphous silicon has been systematically investigated for wide range of implanted species under well-defined experimental conditions. The two main aims of the study have been: (i) to examine the generality of the recrystallization behaviour, particularly the dose dependence, identified for the Pb^+-implanted silicon system, and (ii) to investigate the possible effect[16] of implant species on the epitaxial regrowth process.

A most important part of investigation (i) was the detailed examination of Si^+-implanted silicon, which produces an amorphous surface layer for subsequent

‡ Permanent address: Centro Atomico Bariloche, San Carlos de Bariloche, Rio Negro, Argentina.

annealing studies without any complicating effects due to foreign species. Previous reports[6,10,14,15] have already indicated that the annealing behaviour for the Si^+-implanted silicon system may be qualitatively similar to that observed for Pb^+-implanted silicon. With regard to aim (ii), species chosen for investigation were selected as being representative of a wide range of physical and chemical properties when implanted into silicon (i.e., solubility, chemical reactivity, diffusivity, atomic size and mass). Care has been taken to consider other parameters such as implant concentration and amorphous-layer thickness so that valid species comparisons can be attempted. RBS of 2-MeV He^+ ions and TEM have been the analysis techniques employed to examine the lattice disorder and implant profiles in implanted and annealed ⟨111⟩ silicon.

2 EXPERIMENTAL

The sample preparation and implantation details have been previously described,[1] and only the experimental procedures with special relevance to the current series of experiments will be given here. Sixteen different species were implanted at dose rates $\lesssim 5\ \mu Acm^{-2}$ into ⟨111⟩ silicon targets to a variety of doses and at energies as listed in Table I. The number of discrete doses analysed has been listed in column 3, together with the appropriate dose range. Column 4 lists the types of analyses undertaken, A, B, and C referring to Rutherford backscattering/channeling measurements of lattice disorder, high-resolution (low-angle) RBS measurements of the implanted profile, and TEM, respectively.

The particular details of the RBS and TEM analysis procedures have also been previously described.[1] It is, however, worth reiterating the annealing procedures. All implanted samples were analysed prior to heat treatment and after isochronal annealing steps at 500, 650, and 850°C in flowing dry argon for 30 min. Some of the higher-dose Ni^+-implanted samples were given longer anneals at the higher temperatures to aid silicide formation as identified by TEM.

TABLE I

A summary of the implant and analysis conditions for the implanted ⟨111⟩ Si targets. The implant-dose column lists the number of doses employed and the dose range, whereas column 4 lists the type of analyses performed on each implanted system, A, B, and C, referring to RBS and channeling-disorder measurements, low-angle RBS determination, and transmission microscopy investigation, respectively, as described in the text.

Species	Energy/keV	Doses/ions cm^{-2}	Analysis
N_2^+	15	3: 10^{13}–10^{15}	A
Ne^+	20	3:3 × 10^{14}–3 × 10^{16}	A
Si	15	9: 10^{14}–3 × 10^{16}	A
Ar^+	40	3: 3 × 10^{14}–3 × 10^{16}	A, B, C
Cr^+	20	2: 10^{15}–3 × 10^{16}	A, B
Ni^+	40	5: 10^{13}–10^{17}	A, B, C
Ga^+	20	2: 10^{15}, 8 × 10^{15}	A, B
As^+	30, 40	6: 3 × 10^{14}–3 × 10^{16}	A, B, C
Br^+	30	3: 3 × 10^{14}–3 × 10^{16}	A, B, C
Kr^+	40	5: 10^{13}–3 × 10^{17}	A, B, C
Xe^+	40	5: 10^{13}–3 × 10^{17}	A, B
Cs^+	30	6: 10^{14}–5 × 10^{16}	A, B
Pt^+	20	1: 10^{15}	B
Pb^+	20, 40, 80	18: 2 × 10^{12}–10^{17}	A, B, C
Bi^+	20	1: 10^{15}	B
U^+	20	1: 3 × 10^{15}	A, B

3 RESULTS

3.1 *Residual-silicon Disorder*

The RBS disorder measurements for all species implanted into silicon have indicated the same qualitative dose dependence as was exhibited by the Pb^+-implanted silicon data reported previously:[1] that is, the residual lattice disorder following annealing beyond 600°C increases with increasing implant dose. For example, Figure 1 shows the random and ⟨111⟩ aligned RBS spectra (silicon portion only) for 30-keV As^+-implanted silicon at three doses and illustrates this general behaviour. Figure 1a contains the 3 × 10^{14} As^+ cm^{-2} and 3 × 10^{15} As^+ cm^{-2} spectra and Figure 1b the 3 × 10^{16} As^+ cm^{-2}

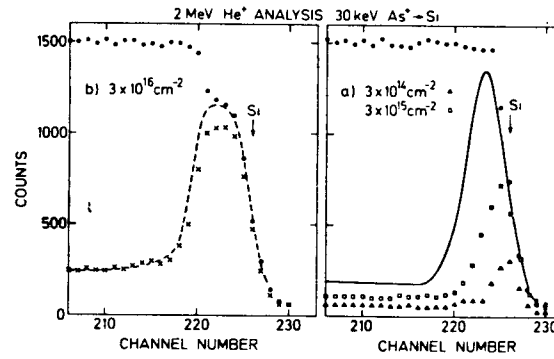

FIGURE 1 2-MeV He^+ backscattered spectra for 30-keV As^+-implanted ⟨111⟩ Si annealed up to 650°C. Random (○) and ⟨111⟩ aligned spectra for three As^+ doses: (a) 3 × 10^{15} cm^{-2} (□) and 3 × 10^{14} cm^{-2} (△); and (b) 3 × 10^{16} cm^{-2} (×). Solid and dashed curves indicate respective aligned spectra prior to annealing.

spectra, after annealing at 650°C for 30 min. The dashed and solid curves represent the respective aligned spectra prior to annealing and were essentially unchanged after annealing at 500°C for 30 min. Similarly, the spectra taken after annealing to 850°C for 30 min were little changed from the 650°C spectra shown in Figure 1a and b, indicating that, for our annealing schedule, reordering proceeds abruptly during the 650°C anneal.

The magnitude of the disorder peak area following a 650°C anneal can be taken as a measure of the residual disorder, which is clearly shown in Figure 1 to increase with increasing As^+ dose. It is important to note that all doses indicated exceed the amorphous threshold. (Here, the amorphous threshold is defined as the dose just sufficient to create a continuous amorphous layer extending from about the ion range back to the silicon surface and for 30-keV As^+ is about 1×10^{14} cm^{-2}.) The difference in shape between the high- and low-dose spectra arises from the increased stopping power of the composite Si/As-implanted layer for the analysing He^+ ions. The effect is for the high-dose random spectrum to exhibit a near-surface dip (lower yield) and for the aligned disorder peak to be correspondingly lower and broader, as shown in Figure 1b. In all cases, the area under the aligned disorder peak (after subtracting a small dechanneling contribution,

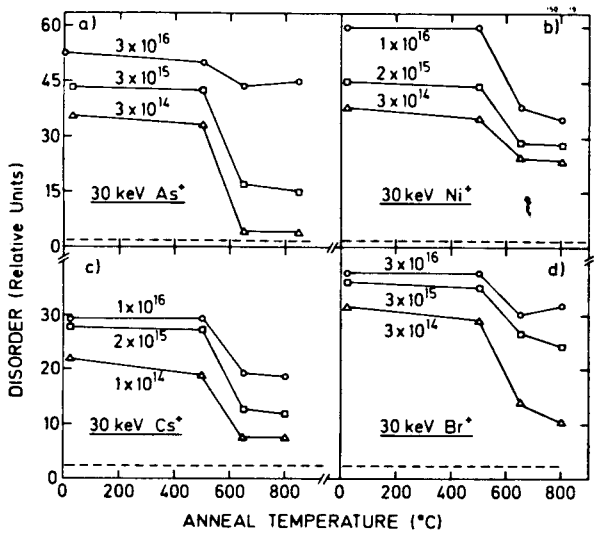

FIGURE 2 Si-lattice disorder (relative units) as a function of annealing temperature obtained from ⟨111⟩ aligned 2-MeV He^+ RBS spectra for 30-keV implantations of (a) As^+, (b) Ni^+, (c) Cs^+, and (d) Br^+ at various doses. Dotted lines in the lower portion of the figures provide a measure of the unimplanted surface-disorder level.

as described previously[1], taken as a measure of the lattice disorder, is plotted for various As^+ doses as a function of annealing temperature in Figure 2a.

The magnitude of the As^+-implanted (20°C) disorder increases slightly with dose even though a completely amorphous layer is obtained for the lowest dose. This effect can be taken to indicate small increases in the amorphous-layer thickness with increasing dose, arising from the disorder created by those implanted ions which penetrate beyond the mean ion range into the tail of the distribution. The magnitude of the residual disorder and the dose dependence of lattice recovery are quantified by considering the 650°C data points of Figure 2a. Shown in Figure 2b, c, and d are similar disorder plots for species Ni^+, Cs^+, and Br^+ implanted into silicon and demonstrate the same general trend for the residual disorder to increase with dose. Similar disorder data have been obtained by RBS for all other implanted impurity species listed in Table I but are not shown here since the results are in qualitative agreement with the dose dependence displayed by the examples presented in Figure 2. The results of the rare-gas implantations into silicon, however, have been reported briefly elsewhere.[7]

An examination of the magnitude of the remnant disorder levels (≳650°C data points) in Figure 2 reveals species differences. For example, a comparison of the low-dose (3×10^{14} cm^{-2}) As^+ and Ni^+ data indicates that the As^+-implanted silicon has recovered almost completely (less than 10% remnant disorder), whereas the Ni-implanted layer has a high (~60%) residual disorder. In this particular case, it is valid to directly compare the As^+ and Ni^+ species effects since, apart from a slight implant-mass difference, the implant and annealing conditions are identical. Differences in amorphous-layer thickness, implant dose and concentration profile complicate species-effect comparisons in the majority of cases and necessitate the adoption of some normalization procedure. Such evaluations are treated in detail in Section 4.2: suffice it to say here that the implant species has been found to influence silicon-lattice recovery at low implant concentrations.

TEM analysis of the systems indicated in Table I showed behaviour essentially similar to that previously observed for the Pb^+-implanted silicon system. The significant findings are summarized in the following points.

i) The structure of the reordered silicon layers exhibited a dose dependence which was qualitatively

similar for all implant systems investigated. With increasing implant dose, the nature of the reordered layer changed from basically bulk-oriented single crystal containing some twinning (doses ~ 3×10^{14} cm^{-2}) to randomly oriented polycrystals (doses $\gtrsim 10^{16}$ cm^{-2}).

ii) Differences between the reordered silicon structure for various implant systems, at similar doses, could be identified. For example, compared with the Pb^+-implanted silicon data, As^+-implanted targets exhibited better single-crystal recovery, and Ni^+ implants resulted in considerably worse recovery (i.e., highly twinned and polycrystalline) at implant doses of 3×10^{14} cm^{-2} in each case.

iii) Evidence for gas-bubble formation in annealed (>600°C) Ar^+- and Kr^+-implanted silicon was found for implant doses exceeding ~5×10^{15} cm^{-2}. Such features may act as nucleation sites for observed poly-crystalline recovery.

iv) Both As^+ and Ni^+ precipitation was observed following annealing of high-dose implants ($\gtrsim 3 \times 10^{16}$ cm^{-2}) of these species. Long-time anneals at high temperatures (e.g., 3 hr at 800°C) for Ni^+-implanted targets for doses $>10^{16}$ cm^{-2} resulted in the formation of stable $Ni\,Si_2$ precipitates.[17]

3.2 Silicon Implantation into Silicon

An additional series of implantations of 15-keV Si^+ into ⟨111⟩ silicon was undertaken for an examination of the dose dependence of residual disorder without the complication of foreign species. Extreme care was exercised to ensure contamination-free implantations. Extensive measurement of the Si^+-isotopic mass ratios (28, 29, 30) indicated that, during implantation, less than 1% of other impurities (mainly N_2^+) were implanted along with Si^+ ions. To determine the scale of the effect on silicon-lattice recovery produced by the impurity, particularly for the highest doses (e.g., 3×10^{16} Si^+ cm^{-2} sample may have 3×10^{14} N_2^+ cm^{-2}), a separate set of ⟨111⟩ silicon control samples were implanted as follows. Three substrates were first implanted with a dose of 5×10^{14} cm^{-2} Si^+ (15 keV), just sufficient to form a continuous amorphous layer and then further implanted with N_2^+ (15 keV) ions to doses equivalent to the maximum N_2^+ impurity expected for the three highest-dose Si^+ implants employed. All samples were annealed isochronally at 500, 650, and 800°C and analysed by RBS after each stage, as described previously.

The random and aligned backscattered spectra for

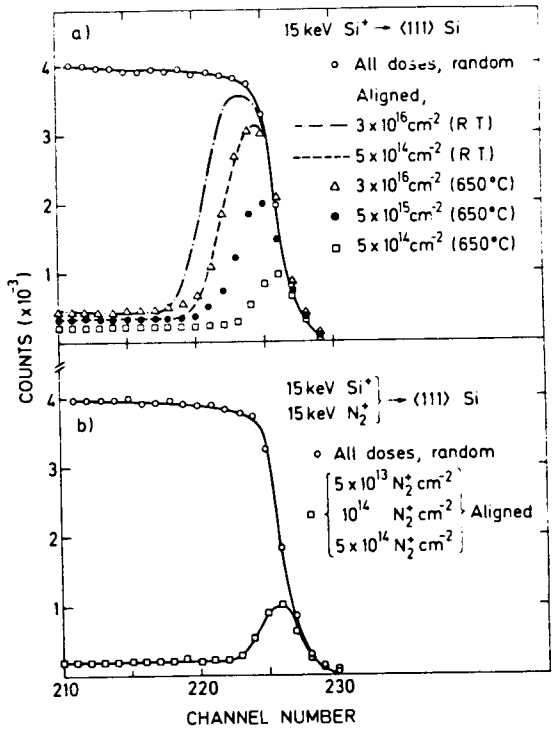

FIGURE 3 Portion of 2-MeV He^+ RBS random and ⟨111⟩ aligned spectra showing relative lattice disorder following 650°C annealing for (a) 15-keV Si^+ implantations into ⟨111⟩ Si and (b) 15-keV Si^+ (5×10^{14} cm^{-2}) and 15-keV N_2^+-implanted ⟨111⟩ Si. Dot-dash and dashed curves in (a) denote the room-temperature spectra for the 3×10^{16} Si^+ cm^{-2} and 5×10^{14} Si^+ cm^{-2} implants.

three doses of Si^+ (5×10^{14}, 5×10^{15}, 3×10^{16} cm^{-2}), after annealing to 650°C, are shown in Figure 3a. The dot-dash and dashed curves indicate the as-implanted aligned spectra for the 3×10^{16} and 5×10^{14} implantations, respectively. The peak area of the 3×10^{16} cm^{-2} as-implanted spectrum is about 25% greater than that at 5×10^{14} cm^{-2}, indicating a corresponding thickening of the amorphous layer into the tail region of the implanted Si^+ distribution, as suggested previously. The aligned peak areas corresponding to the annealed samples again demonstrate the increase in remnant disorder with dose. In Figure 3b, the spectra for the N_2^+-implanted control samples (after annealing to 650°C) are shown and clearly indicate that the small N_2^+ impurity does not produce the high residual-disorder levels of Figure 3a.

The dose dependence of the residual disorder is clearly shown in Figure 4, where all the Si^+-disorder measurements (quantified from disorder peak areas)

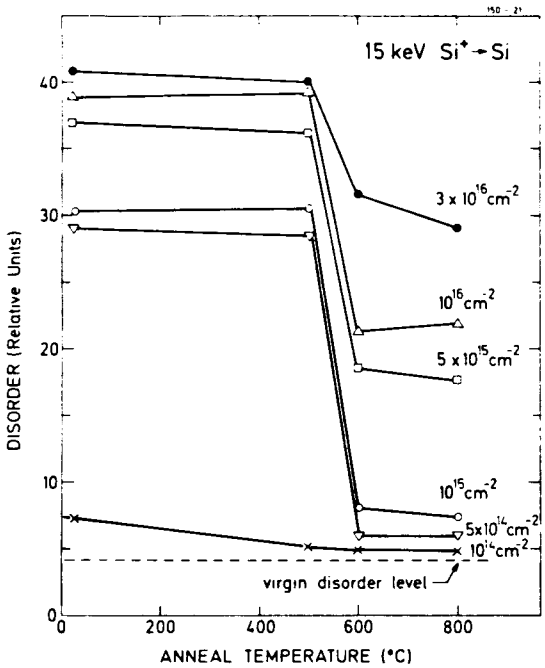

FIGURE 4 Si-lattice disorder as a function of annealing temperature for various doses of Si^+ (15-keV) implantations into ⟨111⟩ Si. Data obtained from peak areas of 2-MeV He^+-aligned spectra similar to those of Figure 3.

are plotted as a function of annealing temperature. Comparison of the residual ($\gtrsim$650°C) disorder levels for Si^+ implants with those of other species is made in Section 4.

3.3 *Implant Redistribution Effects*

Low-angle RBS analysis indicated that, in many cases, a significant redistribution of the implanted species within the silicon surface layers had taken place during annealing. In general, the as-implanted profiles (near-Gaussian in shape for doses $\gtrsim 5 \times 10^{15}$ cm^{-2}) developed a pronounced peak at the near-surface with a reduced yield in the region of the original distribution. This resultant double-peaked structure is illustrated in Figure 5, where the profiles for As^+, Cs^+, Pt^+, and Bi^+ implants in silicon are plotted for the various annealing stages. The depth resolution (three channels) is of the order of 40Å and has been obtained using a low-angle RBS geometry with the incident beam inclined at 5° to the target surface. The near-surface peak obtained after annealing for the profiles illustrated was observed for most implant species investigated and is

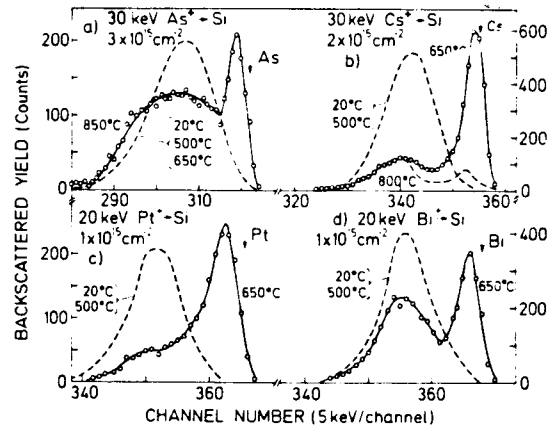

FIGURE 5 Implant profiles obtained from low-angle (5° incidence to target surface) RBS analysis using 2-MeV He^+ ions. (a) 30-keV As^+ (3×10^{15} cm^{-2}). (b) 30-keV Cs^+ (2×10^{15} cm^{-2}). (c) 20-keV Pt^+ (1×10^{15} cm^{-2}). (d) 20-keV Bi^+ (1×10^{15} cm^{-2}).

suggestive of outdiffusion of part of the implant during annealing.

The important similarities and differences in redistribution for the various implants in silicon can be summarized as follows. (The examples of Figure 5 are employed, where applicable, to illustrate the specific observations.)

i) In no instance was any significant implant redistribution observed for anneals below 600°C or before silicon recrystallization, as indicated by TEM. This suggests that the implant outdiffusion may be correlated directly with the recrystallization process or with the nature of the reordered (polycrystalline) layer.

ii) Outdiffusion was only observed in cases where TEM revealed that the implant layer reordered as a polycrystalline network (i.e., only for the higher implant doses), and for most species (Pb^+, Xe^+, Cs^+, etc.), there appeared to be a well-defined threshold dose usually of the order of 10^{15} cm^{-2} below which no outdiffusion was observed during annealing. The magnitude of this threshold dose changed with both implant energy and type. For example, low-energy (near-surface) implants exhibited outdiffusion effects at a lower dose, and some species (e.g., Ni^+, Br^+, and Cr^+) were observed to migrate only for doses in excess of 10^{16} cm^{-2}.

iii) The double-peaked structure of the redistributed profiles shown in Figure 5 was typical of most species in that outdiffusion was usually rapid but never total. Part of the original distribution always remained "trapped" at or beyond the original ion

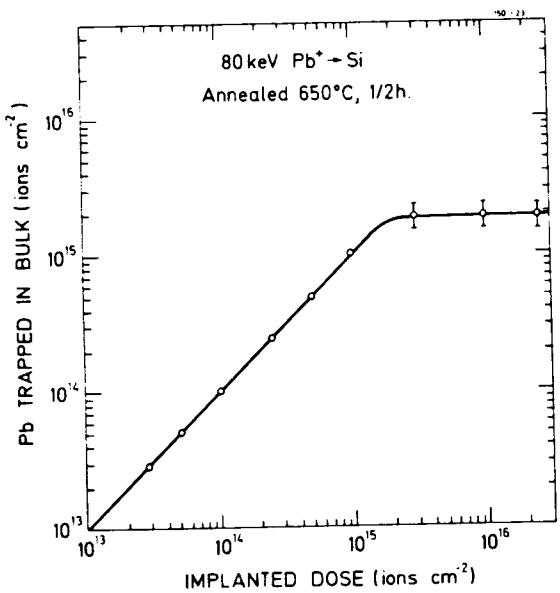

FIGURE 6 The amount of Pb trapped at or beyond the ion range plotted as a function implantation dose after thermal annealing beyond 650°C of ⟨111⟩ Si implanted with 80-keV Pb^+. Data obtained from low-angle 2-MeV He^+ analysis.

range, and the rest migrated out to the target surface. The fraction of the original implant, which remains "trapped" in the bulk, appears to be species-dependent. For species Pb^+, noble gases, Bi^+, Cs^+, Ga^+, Pt^+, and U^+, the absolute trapped amount is practically independent of dose and corresponds closely to the outdiffusion threshold dose of $\sim 10^{15}$ ions cm^{-2} discussed in (ii), whereas the trapped amount of species such as As^+ and Ni^+ increases with dose. The former (dose-independent) behaviour is illustrated for Pb^+ in Figure 6, where the absolute trapped amount is plotted against Pb^+ dose for 80-keV Pb^+ implants in silicon. In some cases (e.g., the As^+ profiles of Figure 5), part of the bulk peak seems to reside slightly deeper than the original distribution, possibly indicating some, small indiffusion.

iv) The temperature at which outdiffusion is observed, while never below 600°C, is species- and dose-dependent. In Figure 5, for example, Cs^+, Pt^+, and Bi^+ exhibit outdiffusion sharply at 650°C, whereas As^+ does not redistribute until annealing at 850°C. Also, Ni^+ was only observed to outdiffuse after long-time (>3 hr) anneals above 800°C and, for the noble gases, the migration temperature changed with dose (concentration) of implant.

v) The outdiffusing species appear, in the majority of cases, to be trapped at or near the target surface, usually behind the residual surface oxide on silicon. Some species do not build up at the surface (e.g., Br^+) but are completely lost, while others are significantly diminished (e.g., Cs^+ in Figure 5) usually after higher-temperature anneals. Furthermore, the surface peak of some species (e.g., Pt^+ in Figure 5) is not sharp and appears to tail into the bulk and merge with the "trapped" fraction. This behaviour can be attributed either to surface precipitation (identified by TEM for Pb^+ and Ni^+ in silicon) or to trapping of some impurity in transit to the surface.

3.4 Asymmetric High-dose Profiles

In examining the high-dose ($\gtrsim 5 \times 10^{15}$ cm^{12}) as-implanted profiles by high-resolution (low-angle) RBS, most of the distributions were found to be asymmetric. In general, the profiles exhibited a flat-top and became skewed towards the target surface as a result of substrate sputtering. However, in some cases, effects which could not be attributable to sputtering were noticed. Such behaviour is typified by the as-implanted Cs^+ profiles shown in Figure 7. The low-dose (5×10^{15} cm^{-2}) profile shows the expected, slight skew towards the surface, but the higher-dose profiles, somewhat unexpectedly, reveal a double peak. One interpretation is that the surface peak is indicative of radiation-assisted outdiffusion. (Heating effects were reduced by cooling the target during implantation.) The shift in the implant peak position to lower backscattered energies for the higher-dose profiles can partly be explained by a

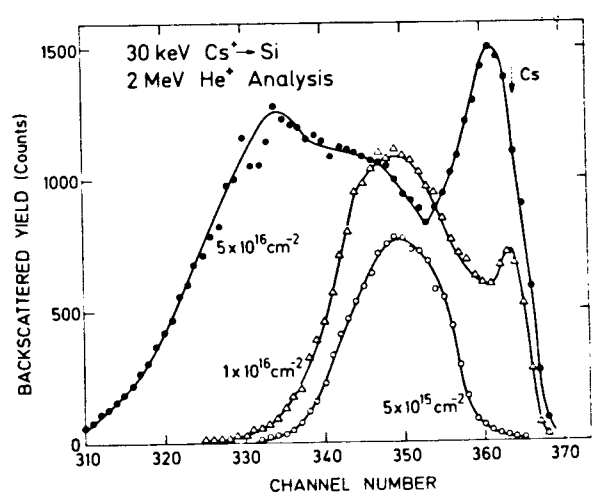

FIGURE 7 30-keV Cs^+ profiles in ⟨111⟩ Si obtained from low-angle (5° incidence to target surface) 2-MeV He^+ analysis.

stopping-power increase for He^+ ions in the composite Si/Cs target. Nevertheless, the shift in the 5×10^{16} Cs^+ cm^{-2} profile seems excessive and may suggest diffusion towards the bulk. Effects similar to those shown for Cs in Figure 7 have also been observed for Pb^+ and Br^+ and are discussed in detail elsewhere.[18]

4 DISCUSSION

4.1 General Recrystallization Effects

The RBS results presented here for the reordering of silicon implanted with many different elemental species confirm the basic generality of the dose dependence of recrystallization both suggested in earlier works[6–8,10] and studied in detail for the Pb^+-implanted silicon system.[1,2] More specifically, the RBS data indicate that the ability of amorphous silicon layers to recover as a single crystal after annealing decreases with increasing implant dose. The data collected for Si^+ implantations into silicon suggest that, qualitatively, this behaviour is independent of ion species although we shall demonstrate in the following section that the type of implant species can influence the degree of silicon-lattice recovery.

The detailed TEM studies undertaken for the Pb^+-implanted silicon system indicated that the magnitude of the RBS residual disorder could be taken as a useful measure of the polycrystallinity within the reordered lattice, whereby increased implant dose resulted in increased misorientation of crystal grains with respect to the underlying bulk lattice. Both additional TEM data of our own (Table I) and those of other workers[9–11,19,20] for many different implant species support this correlation. However, it should be stressed that this interpretation of RBS disorder is only applicable to the isochronal annealing sequence of silicon employed in the current study and should not be inferred for other experimental conditions.

The general nature of the implant-redistribution effects observed in this study suggests that impurity migration can be associated with either the reordering process or the structure of the recrystallized layer. The fact that no outdiffusion was observed in the Pb^+-implanted silicon study until the Pb^+-ion dose was sufficient to result in a polycrystalline reordered layer prompted us to suggest that grain boundaries were acting as easy diffusion paths for the Pb^+ impurity. A similar proposal for In^+ outdiffusion from implanted silicon has recently been put forward by other workers.[13] Thus, the outdiffusion behaviour observed in the present study has been likewise attributed to the presence of grain boundaries within the reordered layer. Outdiffusion effects during silicon recrystallization have been observed by other workers[21,22] for implant doses too low to result in a polycrystalline layer, and the suggestion put forward[21] is that part of the implant is "pushed" ahead of the recrystallization front as it advances epitaxially from the bulk lattice towards the surface. Such effects were not observed in the present study, possibly because the somewhat higher implantation doses used here resulted in a polycrystalline rather than in an epitaxial reordered layer.

The general recrystallization behaviour observed for all species implanted into silicon, especially the implant-dose (concentration) dependence, the polycrystallinity of the reordered layer for high-dose implants and the nature of implant outdiffusion, supports the basic step-by-step representation of the recrystallization process put forward to account for the results of the Pb^+-implanted silicon system (Figure 9 of Ref. 1). During annealing, epitaxial regrowth of the amorphous silicon layer may proceed from the underlying bulk towards the surface. Regrowth is likely to be reasonably good in the initial stages since the impurity concentration is low in the tail of the distribution, but the epitaxial growth becomes increasingly inhibited as the higher-concentration regions of the profile are encountered. For sufficiently high impurity concentrations, the growth of a polycrystalline structure completely dominates epitaxial recovery. Grain-boundary assisted outdiffusion of the impurity is now possible through the polycrystalline region of the reordered layer, but some impurity always remains trapped in the low-concentration tail region of the original profile where single-crystal recovery is partly achieved.

The Si^+-implantation results are consistent with the above recrystallization process and suggest that the origin of the polycrystalline structure for high-dose implants is not necessarily one of nucleation by impurity precipitation or compound formation. Following a recent proposal[3] on the importance of stress effects in high-dose implanted silicon, we speculate here that the epitaxial regrowth may be inhibited by the expected high stresses within the surface layers of heavily implanted silicon. This suggestion will be discussed in more detail in the final article in this series.[23]

4.2 Species Effects

Although the basic silicon-recrystallization behaviour is qualitatively similar for all implant

species investigated, both the RBS and TEM data of Section 3.1 indicate that significant species differences exist in respect to the scale of the observed effects. To quantify such differences, we present the remnant silicon-disorder data, obtained by RBS, for all implant species in Figure 8 and 9. An attempt has been made to isolate the regrowth effects attributable to other implantation parameters so that differences in recrystallization behaviour arising specifically from implant species may be clearly identified. With regard to dose-dependent effects, the data have been divided into three dose regions shown in Figures 8a, b, c, and 9, as indicated by the closed, open, and half-closed symbols for the particular, labelled species. Furthermore, the thickness of the implant-induced amorphous layer (dependent upon implant energy for a particular species) has been employed as abscissa to indicate the influence of this parameter on residual disorder. A slight implant-mass dependence of residual disorder was found but, by presentation of the results for high- and low-mass species on separate figures, this complication was efficiently removed. Thermal history effects are not significant since a similar anneal schedule was employed for all implanted targets.

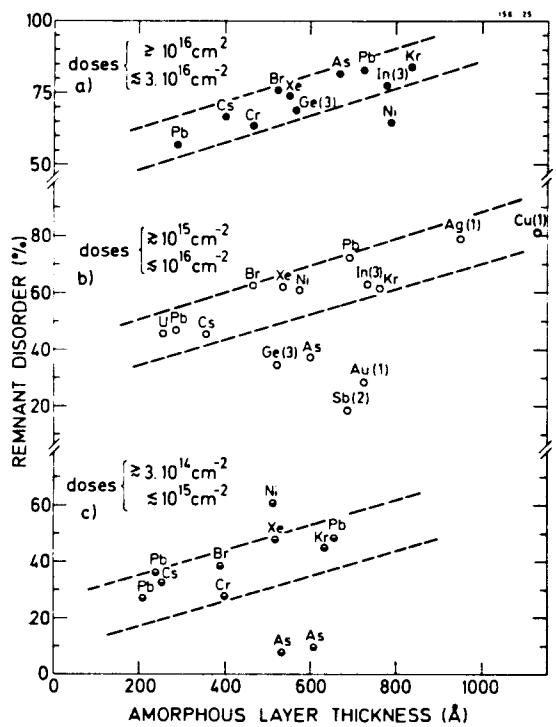

FIGURE 8 Remnant Si-lattice disorder (following annealing to 650°C) plotted as a function of original amorphous-layer thickness for various species implanted into ⟨111⟩ Si. The data have been obtained from 2-MeV He^+ analysis (see text), and three dose regimes are denoted in (a), (b), and (c), as indicated. Only implant species with mass > 40 are plotted, and the particular species are indicated above each data point.

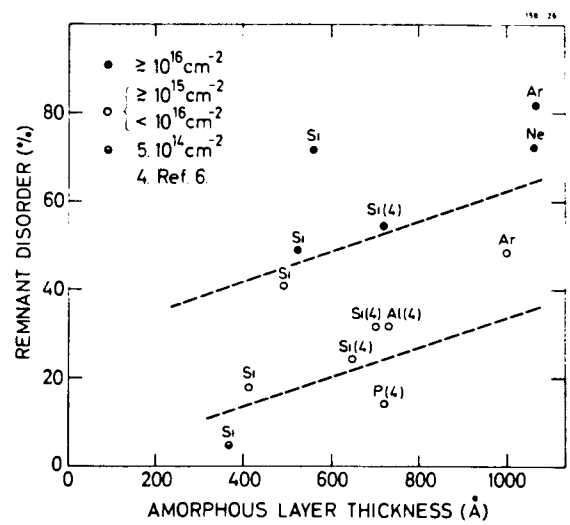

FIGURE 9 Remnant Si-lattice disorder (following annealing to 650°C) plotted as a function of original amorphous-layer thickness for various low-mass species (mass ≤ 40) implanted into ⟨111⟩ Si. Three dose regimes are indicated by the closed, open, and half-closed circles, and data have been obtained from 2-MeV He^+ analysis, as described in the text.

The data points plotted in Figures 8 and 9 were obtained from spectra and plots similar to those of Figure 1 and 2. The magnitude of the as-implanted disorder peak area for a particular dose and species (e.g., As^+ implants in Figure 1) was employed as a relative measure of the amorphous-layer thickness (the abscissa of Figures 8 and 9), with a thick amorphous layer used to obtain an approximate absolute thickness calibration.[24] The corresponding values of the ordinate in Figures 8 and 9 were found by expressing the residual disorder after a 650°C anneal (e.g., Figure 2) as a percentage of the as-implanted disorder. Some data from other workers have been included in the resultant plots, as indicated by the referenced points. The amorphous-layer thicknesses associated with such points have been estimated by comparison with similar mass/energy implants employed in this study. Care was also taken to check that the annealing schedule used to obtain the data corresponded closely with that of this study.[25] It should be emphasized that Figures 8 and 9 are merely an attempt at placing

disorder data from all implant species on a universal plot and, due mainly to possible errors in estimating amorphous-layer thicknesses, should only be useful in indicating overall trends and obvious exceptions rather than showing small absolute differences between species.

An examination of the data embodied in Figures 8 and 9 reveals the influence of several implant parameters on the magnitude of the remnant disorder. Dotted lines have been drawn (somewhat arbitrarily) to bound the regions for each dose regime, where most of the data lie, and, thus, to highlight both the general behaviour and implant-species differences. In particular, the dose dependence (cf. the percentage disorder for the bounded regions, Figure 8a, b, and c), the influence of amorphous-layer thickness (note the slope of the dotted lines), the small implant-mass dependence (cf. absolute disorder from similar dose regimes for Figures 8 and 9) and implant-species effects (cf. species which do not fall within the bounded regions for a particular dose regime) are clearly identified. The parametric equation,

$$D_r = D_r(\text{dose, energy, } M_1, \text{species})$$

conveniently expresses the dependence of residual disorder (D_r) on these parameters, where the amorphous-layer thickness is dependent upon the implant-energy and mass M_1 parameters. We emphasize here that D_r is effectively a measure of the polycrystallinity or average grain misorientation of the reordered layer with respect to the underlying silicon substrate. The differences in recrystallization behaviour attributable to the fourth parameter, implant species, are now examined.

For the highest doses (closed circles), all implant species appear to result in similarly high remnant disorder levels except perhaps Ni^+, where the disorder is significantly lower. This suggests that high implanted Ni^+ concentrations tend to aid silicon recovery as a single crystal compared to other species. It is possible that the formation of Ni Si precipitates, identified by TEM,[17] is responsible for promoting improved silicon recovery, and it is interesting to note, in this regard, that high doses of Pd^+ (also likely to form a silicide with silicon[26]) have been reported to similarly result in somewhat lower levels of residual disorder.[7,10]

Examination of the lower-dose ranges (half-filled and open circles) shows that whereas most species (i.e., U^+, Pb^+, Cs^+, Br^+, Xe^+, Kr^+, In^+, Ag^+, Cu^+, Al^+, Si^+, Ar^+, and Ne^+) fit again into narrow remnant disorder bands, there are more exceptions. For example, the open-circle values for Ge^+, As^+, Au^+, and Sb^+ from Figure 8 and P^+ from Figure 9 appear to be low. Here, it is relevant to note that (for low-impurity concentrations) certain implant species have been reported[27] to enhance or retard epitaxial regrowth rates. In particular, the soluble species such as As^+, P^+, and B^+ were found to significantly enhance regrowth compared with Si^+ implants. This is consistent with the low disorder levels revealed in Figures 8 and 9 for the soluble species Ge^+, As^+, Sb^+, and P^+. A possible explanation for the apparently low Au^+ value (Figure 8) may derive from the fact that Au is known to form a eutectic with silicon at 370°C.[15] For the low-dose region (half-filled circles), the As^+ values are again low compared to the majority of the other data points, but Ni^+ (a notable exception earlier) is somewhat high.

Thus, although the trends for residual disorder to increase with implant dose and amorphous-layer thickness and slightly with implant mass are general for all species, significant differences in the degree of lattice recovery exist for some implant species, particularly at lower implant concentrations. A careful examination of the outdiffusion behaviour reveals similar species differences. For example, species which lie within the guidelines indicating the general behaviour in Figures 8 and 9 (usually species insoluble in silicon) exhibit similar outdiffusion effects, whereas species which were exceptions in terms of degree of remnant disorder (e.g., As^+ and Ni^+) also differ in their diffusion characteristics. However, subtler differences are apparent in the migration behaviour, exemplified by the varying temperatures at which outdiffusion is observed for different doses of the same species. The behaviour obviously warrants more detailed experimental attention but suggests that the ability of an impurity to migrate during or following recrystallization may depend on the physical or chemical state of the species in the silicon lattice (e.g., soluble, precipitate, or compound).

5 CONCLUSIONS

The results obtained for the recrystallization of ion-bombarded ⟨111⟩ silicon layers for a wide range of implanted species show that the ability of the amorphous layer to reorder epitaxially from the bulk as a single crystal decreases with increasing ion dose (concentration). The residual disorder within the recrystallized layer, as measured by RBS, is also

observed to increase with increasing amorphous-layer thickness and to have a slight dependence on the mass of the implant species. TEM analysis indicates that the high levels of residual (RBS) disorder can be interpreted as an amorphous-to-polycrystalline transition. RBS also shows that out-diffusion of a significant fraction of the implant species may occur during or following reordering of the silicon surface layers, and this can be interpreted in terms of a grain-boundary-assisted migration.

Although, qualitatively, this reordering behaviour is independent of implant species, as specifically demonstrated by the Si^+-implant data, important quantitative species differences can be observed. In particular, the "soluble" species (e.g., As^+, Sb^+, P^+) are found to result an improved epitaxial silicon recovery for lower implant concentrations. Of the several competing factors, which can influence recrystallization of implanted silicon, we suggest that residual stress/strain, attributable to the accommodation of high implant concentrations, may play a major role in inhibiting epitaxial recovery, but at lower implant-concentration levels, implant-species effects may be of comparable, or greater, importance. These and other parameters involved in the recrystallization process will be discussed in detail in the final article of this series.[22]

ACKNOWLEDGEMENTS

G. Carter, L. T. Chadderton and J. L. Whitton are thanked for fruitful discussions and comments on the manuscript. The SRC and NATO are gratefully acknowledged for financial support.

REFERENCES

1. J. S. Williams, C. E. Christodoulides, W. A. Grant, R. Andrew, J. R. Brawn and M. Booth, *Rad. Effects* **32**, 55 (1977).
2. C. E. Christodoulides, W. A. Grant and J. S. Williams, *Appl. Phys. Letters* **30**, 322 (1977).
3. J. S. Williams, *Phys. Letters* **60A**, 330 (1977).
4. W. K. Chu, H. Muller, J. W. Mayer and T. W. Sigmon, *Ion Implantation in Semiconductors*, Osaka (1974) (Plenum Press, N. Y., 1975), p. 177.
5. H. Muller, W. K. Chu, J. Gyulai, J. W. Mayer, T. W. Sigmon and T. R. Cass, *Appl. Phys. Letters* **26**, 292 (1975).
6. R. Prisslinger, S. Kalbitzer, J. J. Grob and P. Siffert, J. de Phys. **34**, 85 (1973).
7. H. Kraütle, *Rad. Effects* **24**, 255 (1975).
8. J. S. Williams and W. A. Grant, *Application of Ion Beams to Materials*, Warwich (1975), Publ. Inst., Phys. Ser. 28 (1976), p. 31.
9. L. T. Chadderton and J. L. Whitton, *Rad. Effects* **23**, 63 (1974).
10. M. Matthews, *Rad. Effects* **11**, 167 (1971).
11. R. Truché, C.E.A. Rapport R4595, Saclay (1974).
12. H. Müller, H. Kranz, H. Russel and K. Schmid, *Appl. Phys.* **4**, 115 (1974).
13. P. Blood, W. L. Brown and G. L. Miller, *Ion Implantation in Semi-conductors and Other Materials*, Boulder (1976) (Plenum Press, N.Y., 1977).
14. A. Golanski, A. Fiderkiewicz, W. Rosinski, C. Bauer, R. Brötzschel and W. Rudolph, *Rad. Effects* **25**, 213 (1975).
15. A. Golanski, A. Fiderkiewicz, H. Rzewuski, M. Lefeld-Sosnowska, J. Grötzschel, U. Kreissig, H. Bartsch and J. Grankowski, *Phys. Status Solidi A* **38**, 139 (1976).
16. A. Johansen, B. Svenningsen, L. T. Chadderton and J. L. Whitton, *Application of Ion Beams to Materials*, Warwick (1975), Publ. Inst. Phys., Ser. **28**, (1976), p. 267.
17. M. Booth, Ph.D. thesis, University of Manchester (1976).
18. C. E. Christodoulides, W. A. Grant and J. S. Williams, *Nucl. Instrum. Methods* (in press).
19. S. M. Davidson and G. R. Booker, *Rad. Effects* **6**, 33 (1970).
20. R. A. Moline and A. G. Cullis, *Appl. Phys. Letters* **26**, 551 (1975).
21. J. W. Mayer, L. Eriksson and J. A. Davies, *Ion Implantation in Semiconductors* (Academic Press, London, 1970.
22. D. G. Beanland (private communication).
23. J. S. Williams, G. Carter, C. E. Christodoulides and W. A. Grant (to be published).
24. Using stopping-power tabulations of J. F. Ziegler and W. K. Chu, *Nuclear Data and Atomic Data Tables* **13**, 463 (1974).
25. RBS analysis using 1-MeV He^+ was employed in some cases and, thus, the relative disorder might be expected to be smaller than for 2-MeV He^+ analysis (due to larger critical angles for channeling at lower energies).
26. W. F. Van der Weg, D. Sigurd and J. W. Mayer, *Application of Ion Beams to Metals* (Plenum Press, N.Y., 1974), p. 209.
27. E. W. Kennedy, L. Csepregi, T. Gallagher, J. W. Mayer and T. W. Sigmon, *V Int. Conf. Ion Implantation in Semiconductors and Other Materials* (Boulder, 1976).